

The Dual PI3K/mTOR Pathway Inhibitor GDC-0084 Achieves Antitumor Activity in *PIK3CA*-Mutant Breast Cancer Brain Metastases



Franziska M. Ippen^{1,2}, Christopher A. Alvarez-Breckenridge³, Benjamin M. Kuter¹, Alexandria L. Fink³, Ivanna V. Bihun¹, Matthew Lastrapes⁴, Tristan Penson³, Stephen P. Schmidt⁵, Gregory R. Wojtkiewicz⁶, Jianfang Ning³, Megha Subramanian¹, Anita Giobbie-Hurder⁷, Maria Martinez-Lage⁸, Scott L. Carter⁴, Daniel P. Cahill³, Hiroaki Wakimoto³, and Priscilla K. Brastianos¹

Abstract

Purpose: Previous studies have shown that the PI3K/Akt/mTOR pathway is activated in up to 70% of breast cancer brain metastases, but there are no approved agents for affected patients. GDC-0084 is a brain penetrant, dual PI3K/mTOR inhibitor that has shown promising activity in a preclinical model of glioblastoma. The aim of this study was to analyze the efficacy of PI3K/mTOR blockade in breast cancer brain metastases models.

Experimental Design: The efficacy of GDC-0084 was evaluated in *PIK3CA*-mutant and *PIK3CA* wild-type breast cancer cell lines and the isogenic pairs of *PIK3CA* wild-type and mutant (H1047R/+) MCF10A cells *in vitro*. *In vitro* studies included cell viability and apoptosis assays, cell-cycle analysis, and Western blots. *In vivo*, the effect of GDC-0084 was investigated in breast cancer brain metastasis xenograft mouse models and assessed by bioluminescent imaging and IHC.

Results: *In vitro*, GDC-0084 considerably decreased cell viability, induced apoptosis, and inhibited phosphorylation of Akt and p70 S6 kinase in a dose-dependent manner in *PIK3CA*-mutant breast cancer brain metastatic cell lines. In contrast, GDC-0084 led only to growth inhibition in *PIK3CA* wild-type cell lines *in vitro*. *In vivo*, treatment with GDC-0084 markedly inhibited the growth of *PIK3CA*-mutant, with accompanying signaling changes, and not *PIK3CA* wild-type brain tumors.

Conclusions: The results of this study suggest that the brain-penetrant PI3K/mTOR targeting GDC-0084 is a promising treatment option for breast cancer brain metastases with dysregulated PI3K/mTOR signaling pathway conferred by activating *PIK3CA* mutations. A national clinical trial is planned to further investigate the role of this compound in patients with brain metastases.

Introduction

Brain metastases are the most common intracranial neoplasm in adult cancer patients and are associated with significant mor-

bidity and mortality (1, 2). Advances in systemic therapies and neuroimaging modalities, earlier tumor detection, and longer survival of cancer patients have contributed to an increased incidence of brain metastases (2, 3). Despite the use of multidisciplinary treatment approaches including surgery, stereotactic radiosurgery, and/or whole-brain radiotherapy, the median survival of affected patients still remains poor, ranging from 4 to 18 months (4, 5). As breast cancer accounts for the most common malignancy in women worldwide (6) and the second most frequent primary tumor causing brain metastases (7), the management of affected patients is a growing challenge.

Recent studies have shown that activation of the PI3K pathway occurs in up to 70% of patients with breast cancer brain metastases (BCBM; refs. 8–10). Oncogenic alterations in phosphatidylinositol-4,5-bisphosphate 3-kinase catalytic subunit alpha (*PIK3CA*) lead to enhanced activation of the PI3K/protein kinase B (Akt)/mTOR pathway, which has been shown to promote the development, progression, and treatment resistance of various cancer types, including HER2-positive breast cancer (11). Inhibition of this crucial pathway presents an appealing strategy for the treatment of BCBM. Although numerous inhibitors targeting this pathway have been developed in recent years, there are no FDA-approved PI3K inhibitors for the treatment of brain metastases (12, 13). PI3K/Akt/mTOR pathway inhibitors that have been

¹Cancer Center, Massachusetts General Hospital, Harvard Medical School, Boston, Massachusetts. ²Department of Neurology, Heidelberg University Hospital, Heidelberg, Germany. ³Department of Neurosurgery, Massachusetts General Hospital, Harvard Medical School, Boston, Massachusetts. ⁴Joint Center for Cancer Precision Medicine, Dana-Farber Cancer Institute/Brigham and Women's Hospital, Harvard Medical School, Boston, Massachusetts. ⁵Center for Systems Biology, Massachusetts General Hospital, Harvard Medical School, Boston, Massachusetts. ⁶Department of Radiology, Massachusetts General Hospital, Harvard Medical School, Boston, Massachusetts. ⁷Department of Biostatistics & Computational Biology, Dana-Farber Cancer Institute, Boston, Massachusetts. ⁸Department of Pathology, Massachusetts General Hospital, Harvard Medical School, Boston, Massachusetts.

Note: Supplementary data for this article are available at Clinical Cancer Research Online (<http://clincancerres.aacrjournals.org/>).

Corresponding Author: Priscilla K. Brastianos, Massachusetts General Hospital, 55 Fruit Street, Yawkey 9E, Boston, MA 02115. Phone: 617-724-1074; Fax: 617-643-2591; E-mail: PBRASTIANOS@mgh.harvard.edu

Clin Cancer Res 2019;25:3374–83

doi: 10.1158/1078-0432.CCR-18-3049

©2019 American Association for Cancer Research.

Translational Relevance

Although substantive efforts have been undertaken to optimize multidisciplinary treatment approaches for patients with breast cancer brain metastases, patients still have a dismal overall survival. In recent years, genomic studies have tremendously improved our understanding of actionable molecular targets in patients with breast cancer brain metastases. The PI3K/Akt/mTOR pathway has been shown to be upregulated in a majority of affected patients. However, there are still no approved systemic agents targeting this pathway to date, and drug administration in the central nervous system is complicated by the inherent properties of the blood-brain barrier. In this study, we demonstrate that the brain-penetrant dual PI3K/mTOR inhibitor GDC-0084 significantly inhibits tumor growth in a preclinical model of *PIK3CA*-mutant breast cancer brain metastasis. The results of our study therefore suggest that GDC-0084 might be a promising treatment strategy for patients with *PIK3CA*-mutant breast cancer brain metastases and warrant further validation in clinical trials.

investigated to date have either shown only modest uptake in the brain (14) or have mainly been tested for their efficacy in the context of primary brain tumors (15–19), breast cancer (20) and brain metastases arising from other primary histologies (21–23).

The blood-brain barrier (BBB) poses an additional challenge for drug administration in the central nervous system, as treatment of brain metastases necessitates compounds that are optimized to cross this biologic barrier (22, 24). A PI3K inhibitor that can effectively penetrate the BBB and achieve metabolic stability within the brain presents a promising approach for the treatment of patients with *PIK3CA*-mutant BCBM. GDC-0084 is a dual PI3K/mTOR inhibitor that is specifically optimized to cross the BBB, achieve good metabolic stability within the brain, has low efflux ratios (25) and has recently been shown to achieve significant tumor growth inhibition in preclinical models of glioblastoma and cutaneous squamous cell carcinoma (cSCC; refs. 26, 27). The role of GDC-0084 in brain metastases has not been investigated. To that end, our aim was to investigate the efficacy of this inhibitor in *PIK3CA*-mutant (MT) and wild-type (WT) BCBM *in vitro* and *in vivo*.

Materials and Methods

Cell lines

We used human metastatic breast cancer cell lines that were *PIK3CA*-mutant [JIMT-1 BR-3 (*PIK3CA* C420R; ref. 28); MDA-MB-361 (*PIK3CA* E545K; ref. 29)] and *PIK3CA* wild type (MDA-MB-231 BrM2, BS-004). The isogenic nontumorigenic epithelial breast cell lines MCF10A (parental, *PIK3CA*-WT) and *PIK3CA* (H1047R/+) MCF10A (heterozygous knockin of *PIK3CA*-kinase domain activating mutation, *PIK3CA*-MT) were also used in *in vitro* validation experiments. The HER2 positive and estrogen and progesterone receptor (ER/PR)-negative cell line JIMT-1 BR-3 (HER2⁺, ER/PR⁻) was kindly provided by the laboratory of Dr. Patricia Steeg (NCI, Bethesda, MD) and the cell line MDA-MB-231 BrM2 (HER2⁻, ER/PR⁻) was a generous gift from the laboratory of Dr. Joan Massagué (Memorial Sloan Kettering Cancer Center, New York City, NY). MDA-MB-361 (HER2⁺,

ER/PR⁺) was purchased from ATCC. BS-004 (HER2⁺, ER/PR⁺) was derived from a patient's excised breast cancer brain metastasis. The patient provided written consent. The study was reviewed and approved by the human subjects Institutional Review Board of the Dana-Farber Cancer/Harvard Cancer Center (Boston, MA), and the research performed in accordance with the Declaration of Helsinki. The epithelial breast cell lines MCF10A (HER2⁻, ER/PR⁻) and *PIK3CA* (H1047R/+) MCF10A (HER2⁻, ER/PR⁻) were purchased from Horizon Discovery. JIMT-1 BR-3, MDA-MB-231 BrM2, and BS-004 cells were cultured in DMEM supplemented with 10% FBS and 1% penicillin–streptomycin–amphotericin B. MDA-MB-361 was cultured in L15 supplemented with 20% FBS and 1% penicillin–streptomycin–amphotericin B. The isogenic pairs MCF10A and *PIK3CA* (H1047R/+) MCF10A were cultured in DMEM/F-12 including 2.5 mmol/L L-glutamine and 15 mmol/L HEPES, supplemented with 5% horse serum, 10 µg/mL insulin, 0.5 µg/mL hydrocortisone, 0.1 µg/mL cholera toxin, and 0.2 ng/mL EGF (30). The *PIK3CA* mutation status of all cancer cell lines was confirmed via whole-exome sequencing.

All cell lines were confirmed to be *Mycoplasma* free and were tested throughout the course of the experiments every month (PCR Mycoplasma Detection Kit, abm).

Viral vectors and transduction of cell lines

Cell lines were engineered to express Firefly luciferase and mCherry (FmC) by transduction with the lentiviral construct LV-pico2-Fluc-mCherry (pLV-FmC), which was kindly provided by Khalid Shah (Brigham and Women's Hospital, Boston, MA)/Dr. Andrew Kung (Dana Farber Cancer Institute, Boston, MA). JIMT-1 BR-3 and MDA-MB-231 BrM2 cells were transduced at a multiplicity of infection of 2 in media containing Polybrene (8 µg/mL; EMD Millipore) for 48 hours. Cells were selected with puromycin (7 µg/mL) for 3 days, visualized by fluorescence microscopy for mCherry to confirm successful transduction, and then sorted for mCherry expression using FACS (FACSARIA Cell-Sorting System, BD Biosciences).

PI3K/Akt/mTOR pathway inhibitor

To investigate blockade of the PI3K/Akt/mTOR pathway, the dual PI3K/mTOR inhibitor GDC-0084 was used. GDC-0084 was kindly provided by Genentech. The inhibitor was added at concentrations ranging from 0.25 µmol/L up to 10 µmol/L to cell culture medium with cells plated at 50% to 70% confluency in *in vitro* studies. Controls were incubated with 0.1% DMSO. The dose of GDC-0084 was chosen based on other preclinical studies in brain tumors with PI3K/Akt/mTOR inhibitors (21, 31). GDC-0084 was diluted in DMSO for *in vitro* studies and in a combination of 0.5% methylcellulose and 0.2% Tween 80 for *in vivo* studies.

Cell viability and apoptosis assays

Cells were plated in triplicates for cell viability assays and in quadruplicates for apoptosis assays at a density of 5,000 cells per well on a 96-well plate. Cell lines were treated with GDC-0084 the next day in concentrations ranging from 0.25 µmol/L to 10 µmol/L for 10 hours (apoptosis assays) and 72 hours (cell viability assays). Controls were incubated with 0.1% DMSO. After treatment, cells were lysed using the Caspase-Glo 3/7 (Promega, apoptosis assays) or the CellTiter-Glo (Promega, cell viability assays) reagent. The luminescence generated by these reagents is proportional to the caspase-3/7 activity or the amount of viable

Ippen et al.

cells respectively, and was read using a Synergy HT multi-detection microplate reader (BioTek). The percentage of caspase-3/7 or viable cells was calculated relative to DMSO-incubated controls.

Cell-cycle analysis

Cells were plated in triplicates at a density of 3.5×10^5 in 60-mm well plates and treated with GDC-0084 (control, 1, 2.5, 5, 7.5, and 10 $\mu\text{mol/L}$) the next day for a total of 72 hours. Afterwards, floating and adherent cells were harvested, washed with PBS, and fixed in ice-cold 70% ethanol for 24 hours. Subsequently, cells were washed with PBS again. Fixed cells were stained using the Propidium Iodide Flow Cytometry Kit (ab139418, Abcam) with 200 μL of propidium iodide (PI) staining solution (500 μL 20 \times PI and 50 μL 200X RNase in 9.45 mL PBS) and incubated at 37°C in the dark for 30 minutes. The cell-cycle analysis was conducted using the BD LSRII and BD FACSDiva Software Version: 8.0.1 (BD Biosciences) and analyzed using FlowJo software version 10 (LLC).

Western blots

Cells were plated in triplicates in 60-mm well plates at a density of 3.5×10^5 cells and treated with GDC-0084 (control, 1, 2.5, 5, 7.5, and 10 $\mu\text{mol/L}$) the next day for a total of 6 hours. Afterwards, cells were harvested and lysed in RIPA buffer (Thermo Fisher Scientific) containing protease and phosphatase inhibitor cocktails (Roche). Twenty micrograms of protein per lane was separated by 4% to 15% SDS-PAGE (Bio-Rad) and then transferred to polyvinylidene difluoride membranes (Bio-Rad) by electroblotting. Membranes were blocked with 5% nonfat dry milk in TBST (20 mmol/L Tris pH 7.5, 150 mmol/L NaCl, 0.1% Tween 20) for 1 hour at room temperature and then incubated with primary antibodies [pAkt (Ser473) #4060, Akt #9272, p-p70 S6 Kinase (Thr389) #9205, p70 S6 Kinase #2708, p-p44/42 MAPK (Erk1/2) (Thr202/Tyr204) #4370, p-MEK1/2 (Ser217/221) #9154, p-p90RSK (Ser380) #11989, p-MSK1 (Thr581) #9595, β -actin #3700, all from Cell Signaling Technology] at 4°C overnight. Membranes were washed with TBST and incubated with horseradish peroxidase-conjugated secondary antibodies [anti-rabbit IgG (H+L), HRP conjugate and anti-mouse IgG (H+L), HRP conjugate, both from Promega] for 1 hour at room temperature. Thereafter, membranes were washed again in TBST and signals were visualized with an ECL blotting substrate (Thermo Fisher Scientific). Blots were analyzed using Image Lab (Bio-Rad) and cropped in Adobe illustrator software version CC 2018.

Animal studies

All *in vivo* mouse experiments were approved by the Institutional Animal Care and Use Committee at Massachusetts General Hospital (Boston, MA).

Stereotactic intracranial tumor implantation. A total of 32 animals were analyzed for imaging (8 animals per cohort) and a total of 4 animals in a separate cohort were analyzed for IHC. Prior to surgery, 8-week-old female athymic nu/nu mice (Charles River Laboratories) were anesthetized with pentobarbital (intraperitoneal injection, 40–70 mg/kg). Anesthetized mice were placed into a stereotactic apparatus and the head was stabilized by the ear bars. After opening the skin over the skull, Bregma was identified, and a total of 10×10^4 JIMT-1 BR-3 cells or 7.5×10^4 MDA-MB-231 BrM2 cells in 4 μL Hanks' Balanced Salt Solution were stereotactically implanted into the right striatum (2 mm lateral

from Bregma, 2.5 mm deep) with a Hamilton syringe. We chose these two cell lines because they have similar growth patterns and doubling times. Afterwards, the skull was sealed with bone wax and the wound was sutured. Postoperatively, all mice were provided carprofen (MediGel CPF, 2-oz cup, Clear H₂O) for a total of 3 days.

Bioluminescent imaging and analysis of tumor burden. Seven days after the surgical procedure, mice were imaged for the first time via bioluminescent imaging (BLI). Dynamic imaging was performed to assess their initial tumor burden. Before undergoing this imaging procedure, mice were anesthetized with isoflurane and injected with 4.5 mg D-luciferin diluted in 300 μL PBS. Ten minutes after injection of luciferin, up to five animals at a time were imaged on the Spectral Ami HTX (Spectral Instruments Imaging). Luminescent exposure times of 60, 1, and 0.5 seconds at 5 minutes intervals were chosen until the peak luminescent signal from the whole mouse body was reached. The tumor burden was analyzed by subtracting the background signal from the signal above the mouse's cranium and measured in total flux (p/s) with the software Aura version 2.2.1.0 (Spectral Instruments Imaging). Figures were generated with the software Amira version 5.3.2 (Thermo Fisher Scientific) using the binning 2, 0.5-second exposure and background subtracted image. To ensure accurate measurement of tumor burden throughout the entire study, mice received a baseline dynamic BLI scan 7 days after tumor inoculation. Mice harboring intracranial tumors with a similar tumor burden and a minimum flux of 10,000,000 p/s in JIMT-1 BR-3 tumors and of 400,000 p/s (flux) in MDA-MB-231 BrM2 tumors were selected for further experiments. Mice were subsequently randomized to GDC-0084 or sham treatment, which was initiated the day after (day 8 postimplantation). BLI-based tumor burden on day 7 (pretreatment) was not statistically different between the GDC-0084 treatment and sham groups. Afterwards, BLI was performed on a weekly basis until the end of the study at 35 days postintracranial tumor implantation to monitor tumor growth in all mice, as measured by flux (p/s). Because of the large magnitude of the total flux(p/s) values, all data were \log_{10} -transformed prior to analysis. The primary endpoint of this study was the difference in tumor burden measured in total photon flux (p/s) between the cohorts that received GDC-0084 versus sham over a period of 35 days. This period was chosen to avoid reductions in BLI signals due to necrosis and therefore, an underestimation of the actual tumor burden as a result (32).

Treatment and monitoring. The dual PI3K/mTOR inhibitor GDC-0084 was administered daily via oral gavage (15 mg/kg) for a total of 28 days. Mice randomized to treatment received 15 mg/kg GDC-0084 diluted in 0.5% methylcellulose and 0.2% Tween 80 per day, mice randomized to sham received a weight-adapted dose of 0.5% methylcellulose and 0.2% Tween 80 daily. Mice were monitored daily following stereotactic intracranial tumor injection and sacrificed at $\geq 20\%$ weight loss, the onset of neurologic symptoms or at the end of the study, which was no later than 35 days postimplantation. In the separate mouse cohort that was analyzed for IHC, brains were harvested 14 days after intracranial tumor cell implantation and after 7 daily dosings.

IHC

Mouse brains were fixed in 10% formalin for 24 hours and subsequently embedded in paraffin. For IHC, 5- μm thick sections

were deparaffinized. Manual staining was conducted for pAkt and pS6 ribosomal protein. For pAkt and pS6 ribosomal protein staining, sections were treated with sodium citrate (pH = 6) and heated for 10 minutes for antigen unmasking. Sections were blocked with TBST/5% normal goat serum (NGS) and incubated in the following primary antibodies overnight: pAkt ((Ser473) #4060, 1:50) and pS6 ribosomal protein [(Ser235/236) #4858, 1:400, both from Cell Signaling Technology]. The next day, sections were alternately washed in TBS and TBST and then incubated with the secondary antibody SignalStain Boost IHC Detection Reagent (HRP, Rabbit, #8114, Cell Signaling Technology) for 30 minutes at room temperature. Afterwards, slides were stained with DAB (Dako) and counterstained with hematoxylin. Automated staining was conducted for p-p44/42 MAPK and pMEK1/2. Sections were treated with prediluted cell conditioning solution (CC2, Ventana), heated for 64 minutes, and blocked in inhibitor CM (Ventana). Sections were incubated with the primary antibody p-p44/42 MAPK [Erk1/2; (Thr202/Tyr204) #4370, 1:500] or p-MEK1/2 [(Ser221) #2338, 1:50, both from Cell Signaling Technology] for 36 minutes and then with the secondary antibody OmniMap anti-Rb HRP (Multimer HRP, Ventana) for 12 minutes. Sections were then stained with DAB (Dako), counterstained with bluing reagent (Ventana) and post-counterstained with hematoxylin.

Statistical analysis

Statistical analysis was conducted with GraphPad Prism version 7 (GraphPad Software) and SAS 9.4 (SAS Institute Inc.) for the mixed effects models. Graphs were cropped with the Adobe Illustrator software version CC 2018. Evaluation of the efficacy of GDC-0084 *in vivo* was calculated by autoregressive linear mixed models. The outcome data of the treatment cohorts (GDC-0084 vs. sham), measured in total flux (p/s), were first log₁₀ transformed. Differences between the treatment cohorts over time were assessed using linear mixed effects models, with an autoregressive covariance structure within mouse. Log₁₀-transformed fold changes in flux were the dependent variable in the mixed model. Independent predictors were treatment, time, and their interaction. A *P* value of <0.05 was considered statistically significant in our analysis.

Results

The dual PI3K/mTOR inhibitor GDC-0084 inhibits cell proliferation and phosphorylation of Akt and p70 S6 kinase in *PIK3CA*-mutant breast cancer cell lines

We used metastatic *PIK3CA*-mutant and *PIK3CA* wild-type BCBM cell lines to investigate the antitumor efficacy of GDC-0084. We first performed *in vitro* assays to assess the survival of adherent *PIK3CA*-MT and *PIK3CA*-WT cell lines in response to increasing concentrations of GDC-0084.

GDC-0084 led to a considerable decrease in the proportion of viable cells (80%–95%) after 72 hours of treatment in *PIK3CA*-MT cell lines (JIMT-1 BR-3, MDA-MB-361), whereas a more modest decrease in viable cells (40%–60%) was observed in *PIK3CA*-WT cell lines (MDA-MB-231 BrM2, BS-004; Fig. 1A).

To determine whether this effect was mediated by apoptosis, Caspase-Glo 3/7 assays were conducted. The dual PI3K/mTOR inhibitor robustly increased caspase-3/7 activity in JIMT-1 BR-3 and MDA-MB-361 cells after 10 hours of treatment, but no such

effect was seen in the MDA-MB-231 BrM2 and BS-004 cell lines (Fig. 1B).

Consistent with these findings, GDC-0084 also strongly inhibited phosphorylation of Akt and p70 S6 kinase in a dose-dependent manner in both *PIK3CA*-MT cell lines over a treatment course of 6 hours (Fig. 1C). In contrast, no significant changes in phosphorylation of Akt and p70 S6 kinase were observed in response to increasing concentrations of GDC-0084 in the *PIK3CA*-WT cell lines over the same treatment duration.

We next used isogenic *PIK3CA*-MT and *PIK3CA*-WT epithelial breast cell lines to determine whether activating mutation of *PIK3CA* confers sensitivity to GDC-0084. GDC-0084 substantially decreased the proportion of viable cells (90%–95%) in *PIK3CA*-MT (H1047R/+) MCF10A cells compared with the *PIK3CA*-WT MCF10A cells (60%–65%) after 72 hours of treatment (Fig. 2A). Correspondingly, GDC-0084 greatly increased caspase-3/7 activity in the *PIK3CA*-MT (H1047R/+) MCF10A cell line, whereas a weaker effect was seen in the *PIK3CA*-WT parental cell line MCF10A (Fig. 2B). The highest apoptotic signal was obtained after 24 hours of treatment.

Previous studies have demonstrated that inhibition of components of the PI3K/Akt/mTOR pathway can lead to compensatory upregulation of the Ras/Raf/MAPK signaling cascade in cancer cells (33, 34). To test whether dual PI3K/mTOR pathway might affect activation of the MAPK pathway in the context of BCBM, we assessed phosphorylation of p44/42 MAPK (Erk1/2), MEK1/2, p90RSK, and MSK1 by Western blots. We did not observe any significant differences in expression levels of p-p44/42 MAPK (Erk1/2), p-MEK1/2, p-p90RSK, and p-MSK1 between *PIK3CA*-MT (Supplementary Fig. S1A) and -WT BCBM cell lines (Supplementary Fig. S1B). In addition, there was also no detectable change in expression of p-p44/42 MAPK (Erk1/2), p-MEK1/2, p-p90RSK, and p-MSK1 in response to treatment with GDC-0084 compared with sham in *PIK3CA*-MT and -WT cells.

Thus, GDC-0084 selectively inhibited the PI3K/Akt/mTOR pathway and induced apoptotic cell death in *PIK3CA*-MT cell lines.

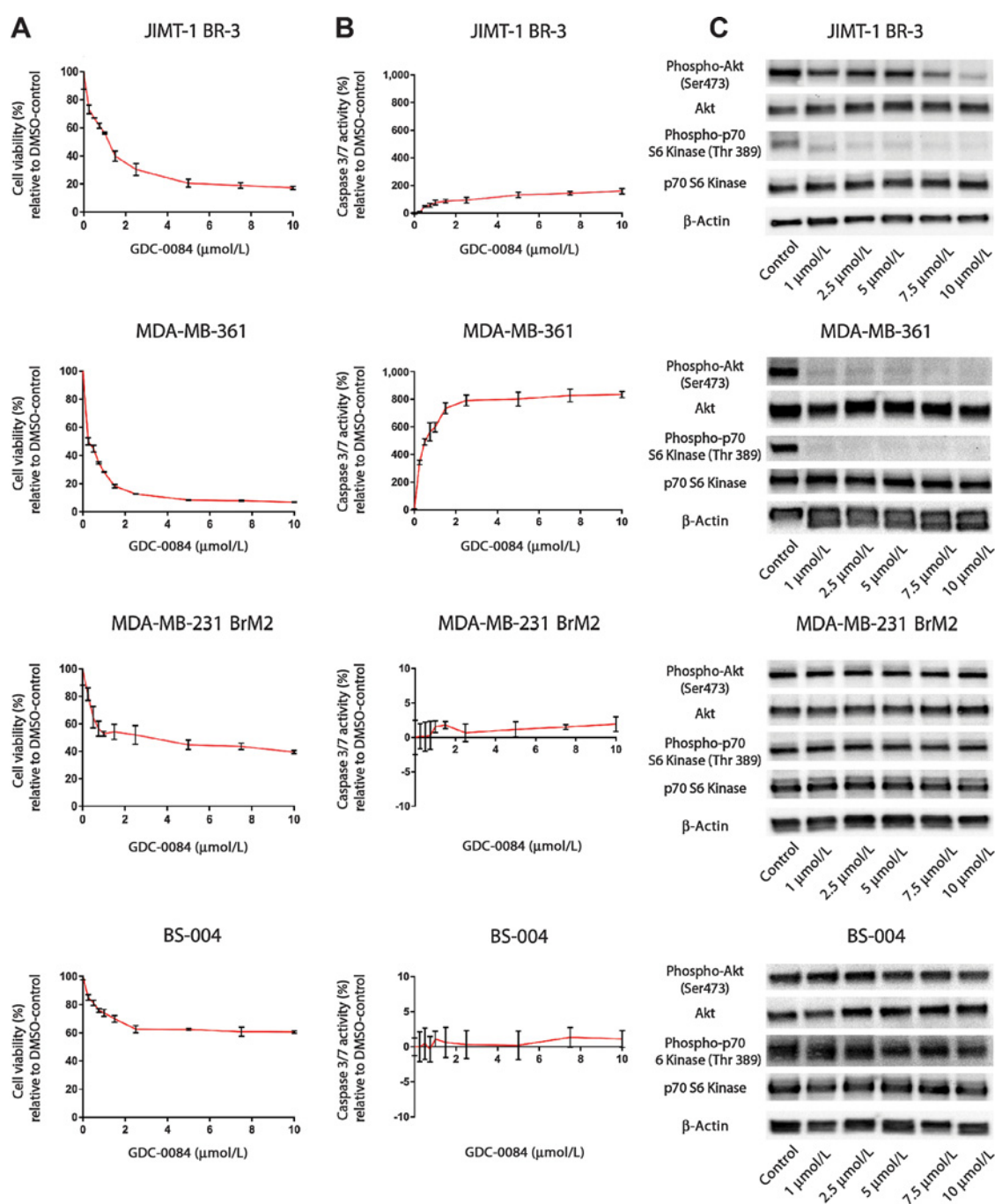
GDC-0084 induces apoptosis in *PIK3CA*-mutant breast cancer cells but not *PIK3CA* wild-type breast cancer cells

To further investigate the reduction in cell viability in *PIK3CA*-MT cell lines, cell-cycle analysis with PI-staining was conducted on all BCBM cell lines. In both cell lines harboring *PIK3CA* mutations, treatment with GDC-0084 for 72 hours yielded a dose-dependent increase in the sub-G₁-phase (apoptotic cells) to approximately 70% in JIMT-1 BR-3 (Fig. 3A and C) and 80% in MDA-MB-361 (Fig. 3C; Supplementary Fig. S2A). For MDA-MB-231 BrM2 (Fig. 3B and C), a mild trend toward an increase in the G₁-fraction was observed, indicative of growth inhibition. GDC-0084 did not induce noticeable changes in cell-cycle phases in BS-004 (Fig. 3C; Supplementary Fig. S2B). This corroborates our *in vitro* findings that GDC-0084 selectively induces apoptosis in *PIK3CA*-MT cell lines.

GDC-0084 significantly inhibits growth of *PIK3CA*-mutant tumors in a patient-derived xenograft brain metastasis model

To investigate whether GDC-0084 can effectively inhibit tumor growth in the brain *in vivo*, we orthotopically implanted either a *PIK3CA*-MT, trastuzumab-resistant (35) cell line (JIMT-1 BR-3) or a control *PIK3CA*-WT cell line (MDA-MB-231 BrM2) into the right striatum of female nude mice.

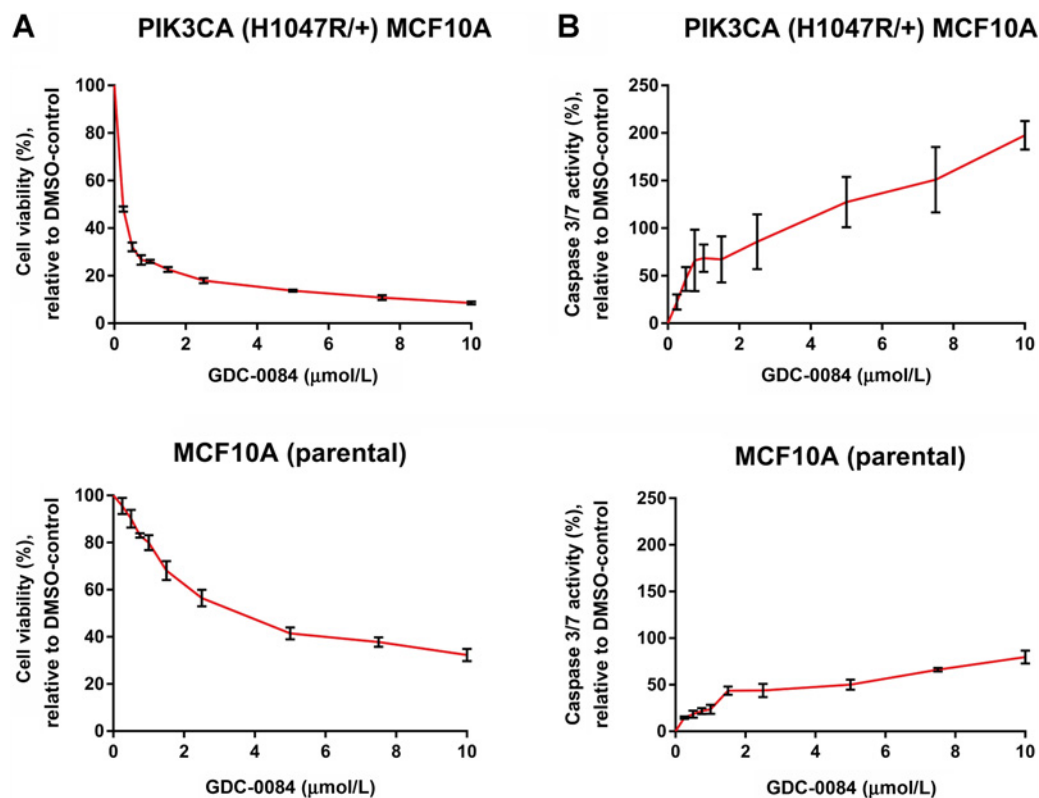
Ippen et al.

**Figure 1.**

The dual PI3K/mTOR inhibitor GDC-0084 selectively reduces cell viability and induces apoptosis in the *PIK3CA*-mutant cell lines JIMT-1 BR-3 and MDA-MB-361 compared with the *PIK3CA* wild-type cell lines MDA-MB-231 BrM2 and BS-004. **A** and **B**, CellTiter Glo cell viability assays after 72 hours of treatment (**A**) and caspase-3/7 Glo apoptosis assays after 10 hours of treatment (**B**) of the breast cancer brain metastases cell lines JIMT-1 BR-3, MDA-MB-361, MDA-MB-231 BrM2, and BS-004 in increasing concentrations with the dual PI3K/mTOR inhibitor GDC-0084. Percentage of growth inhibition is compared with 0.1% DMSO-incubated controls. Error bars represent SEM of cells seeded in triplicates and treated with the same dose. **C**, Western blot analysis of pAkt (Ser473), Akt, p-p70 S6 Kinase (Thr389), and p70 S6 Kinase in JIMT-1 BR-3, MDA-MB-361, MDA-MB-231 BrM2, and BS-004 cell lines treated with GDC-0084 in increasing concentrations for a total of 6 hours. β-Actin was used as a loading control. Western blots are representative of three independent experiments per cell line.

Over the course of the treatment period (28 days), GDC-0084 was well tolerated and no adverse toxicities were observed. In the *PIK3CA*-MT JIMT-1 BR-3 model, BLI of tumor volume 7 days after

the initiation of treatment demonstrated GDC-0084-mediated growth inhibition of tumors, while sham-treated tumors rapidly grew (Fig. 4A). Throughout the duration of the study, GDC-0084

**Figure 2.**

GDC-0084 significantly decreases cell viability and induces apoptosis in the *PIK3CA*-mutant epithelial breast cell line *PIK3CA* (H1047R/+) MCF10A compared with the isogenic *PIK3CA* wild-type parental epithelial breast cell line MCF10A. **A** and **B**, CellTiter Glo cell viability assays after 72 hours of treatment (**A**) and caspase-3/7 Glo apoptosis assays after 24 hours of treatment (**B**) of the epithelial breast cell lines *PIK3CA* (H1047R/+) MCF10A and MCF10A in increasing concentrations with the dual PI3K/mTOR inhibitor GDC-0084. Percentage of growth inhibition is compared with 0.1% DMSO-incubated controls. Error bars represent SEM of cells seeded in triplicates and treated with the same dose.

achieved highly significant inhibition in JIMT-1 BR-3 intracranial tumors (mixed effect model, $P = 0.0004$ for effect of treatment; $P = 0.0005$ for effect of time).

In contrast, no therapeutic benefit of GDC-0084 was noted in the *PIK3CA*-WT MDA-MB-231 BrM2 xenograft model. Intracranial tumors continued to grow rapidly over time in both the sham and GDC-0084 cohorts (Fig. 4B). Accordingly, no significant differences between the two treatment cohorts were detected ($P = 0.80$) and bioluminescent flux increased over time regardless of treatment ($P < 0.0001$).

GDC-0084 inhibits PI3K/Akt/mTOR signaling in *PIK3CA*-mutant breast cancer in the brain

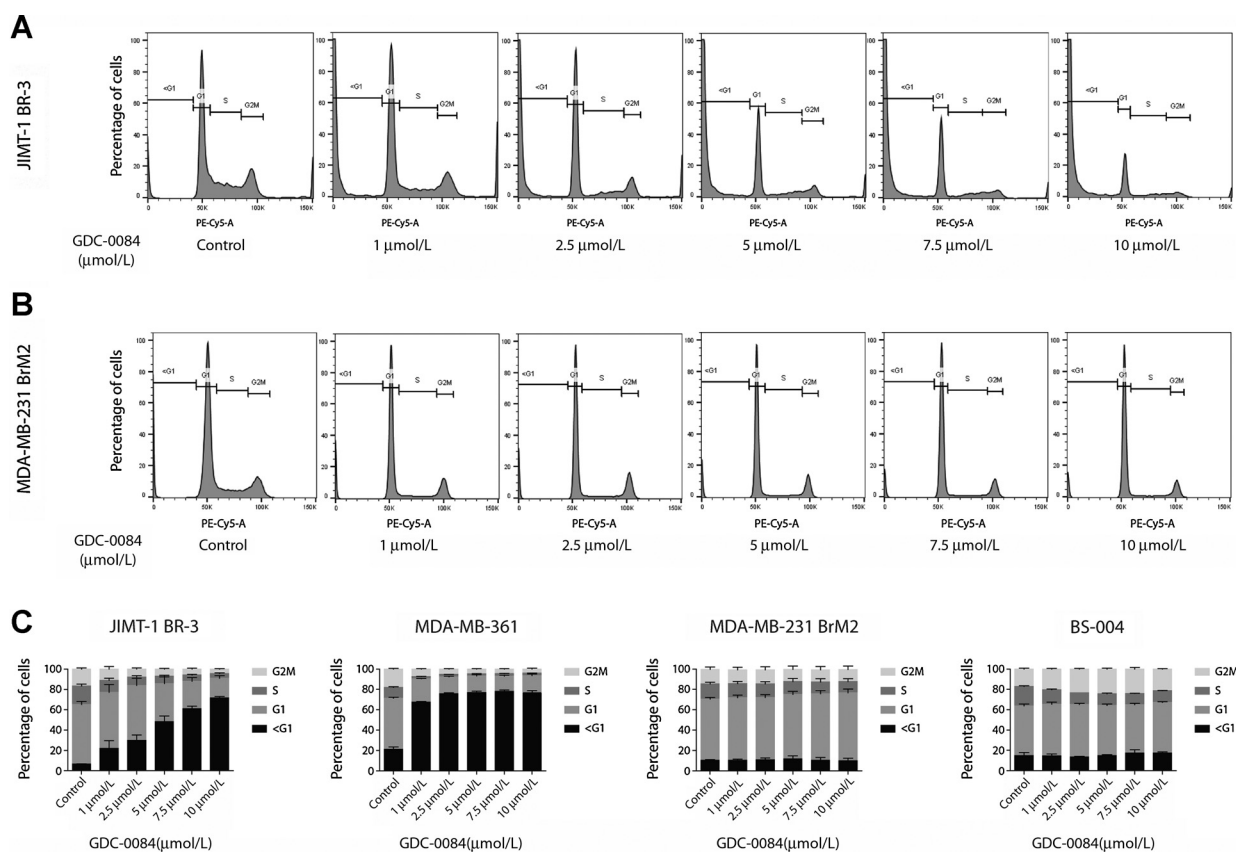
To assess whether GDC-0084 inhibited downstream molecular components of the PI3K/Akt/mTOR pathway in mouse brains, expression of pAkt and pS6 ribosomal protein was evaluated with IHC. In *PIK3CA*-MT JIMT-1 BR-3 tumors, diminished immunostaining of both pAkt (Ser473) and pS6 ribosomal protein (Ser235/236) was observed in the mouse brains treated with GDC-0084 as compared with those of the sham-cohort (Fig. 5). This reduction in signal intensity was consistent with the phosphorylation inhibition seen in GDC-0084-treated *PIK3CA*-MT cell lines *in vitro*, and corroborates the observed tumor growth inhibition *in vivo*. In mice harboring *PIK3CA*-WT MDA-MB-231 BrM2 intracranial tumors, pAkt (Ser473) positivity was sparse,

which was not altered by GDC-0084, and strong pS6 ribosomal protein was only slightly diminished by GDC-0084 treatment (Fig. 5). Collectively, systemic treatment with GDC-0084 potentially inhibited PI3K/Akt/mTOR pathway signaling and tumor growth in intracerebral xenografts generated with *PIK3CA*-MT breast cancer cells. To evaluate whether dual PI3K/mTOR blockade results in pro-survival activation of the Ras/Raf/MAPK pathway as reported previously (33, 34), expression of p-p44/42 MAPK (Thr202/Tyr204) and pMEK1/2 (Ser221) was assessed with IHC. In *PIK3CA*-MT JIMT-1 BR-3 intracranial tumors, pMEK1/2 was negative in both treatment and sham cohorts, and p-p44/42 MAPK was comparably positive in both cohorts (Supplementary Fig. S3). *PIK3CA*-WT MDA-MB-231 BrM2 brain tumors were negative for both p-p44/42 MAPK and pMEK1/2 regardless of treatment (Supplementary Fig. S3). In summary, we did not detect compensatory activation of the Ras/Raf/MAPK pathway after treatment with GDC-0084 *in vivo*, in accordance with our *in vitro* results.

Discussion

Up to 50% of patients with HER2-positive breast cancer will develop brain metastases during their course of disease (36). To date, few effective targeted treatment options are available for patients with BCBM. Genomic studies of matched brain

Ippen et al.

**Figure 3.**

GDC-0084 induces apoptosis in the *PIK3CA*-mutant cell lines JIMT-1 BR-3 and MDA-MB-361 and growth inhibition in the *PIK3CA* wild-type cell lines MDA-MB-231 BrM2 and BS-004. The four breast cancer brain metastases cell lines were treated in increasing concentrations with GDC-0084 for 72 hours, stained with propidium iodide (PI) and underwent subsequent cell-cycle analysis on the LSRII. The cell cycle for JIMT-1 BR-3 (A) and MDA-MB-231 BrM2 (B), treated in increasing concentrations of the inhibitor, is displayed as a histogram. Each phase of the cell cycle (<math><G1</math>, G1, S, G₂M) is gated on the histogram. C, Dose-dependent percentages of phases of the cell cycle were assessed in three independent experiments for each cell line (JIMT-1 BR-3, MDA-MB-361, MDA-MB-231 BrM2, and BS-004) and displayed in a vertical bar graph. All calculations are relative to 0.1% DMSO-incubated controls. Error bars represent SEM of each phase of the cell cycle. See Supplementary Fig. S2 for cell-cycle analysis for MDA-MB-361 and BS-004.

metastases and primary tumors (9, 10) as well as IHC analyses (8), have shown that the PI3K/Akt/mTOR pathway is upregulated in up to 70% of brain metastases in affected breast cancer patients. Targeting this pathway might represent a promising treatment option. To this end, we investigated the antitumor efficacy of the dual PI3K/mTOR inhibitor GDC-0084, which has been shown to cross the BBB and to achieve good metabolic stability in the brain (25). A phase I trial on GDC-0084 in patients with progressive or recurrent high-grade glioma was recently completed (NCT01547546) with FDG-PET data showing that GDC-0084 is able to cross the BBB in humans and achieves a homogeneous distribution in the brain. Furthermore, 18.5% (5/27) of evaluable patients showed a metabolic partial response (37).

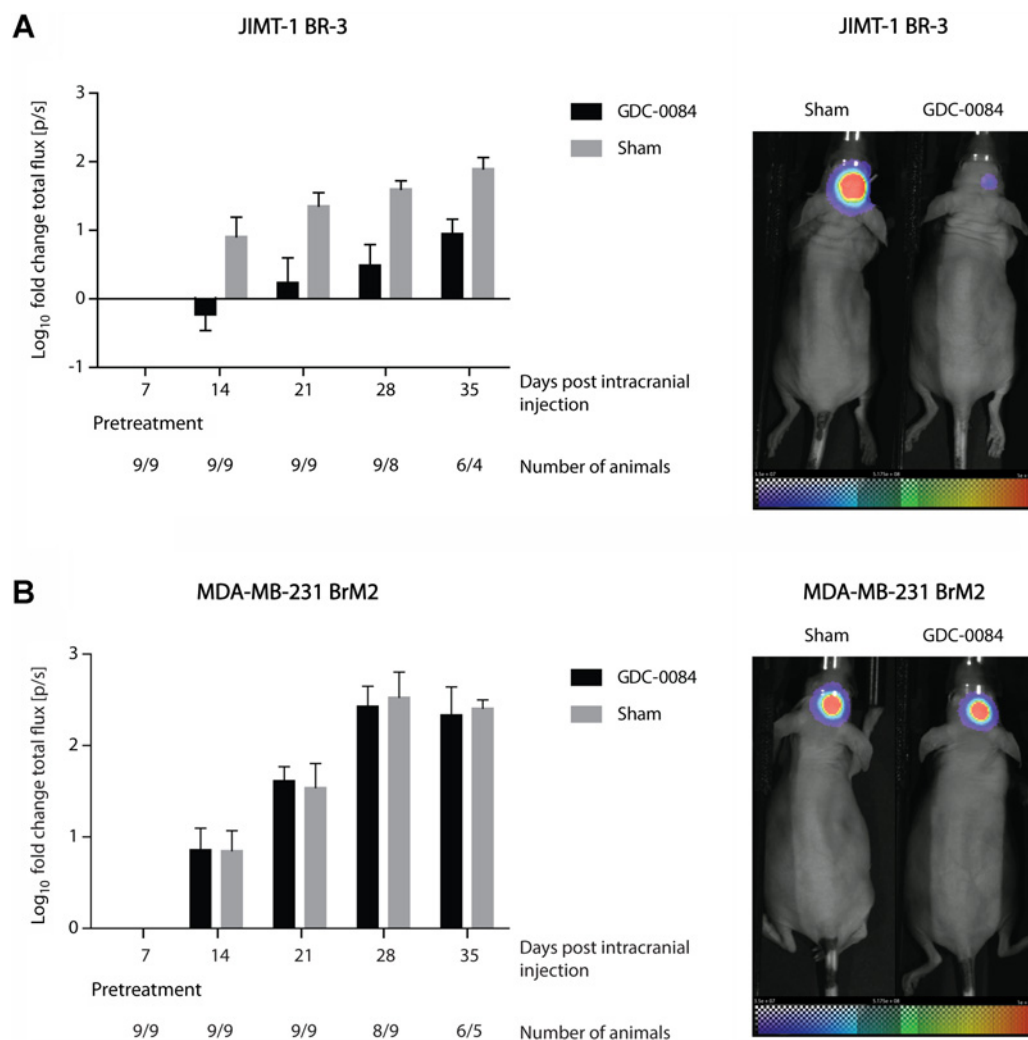
Phase II trials are currently evaluating the efficacy of the PI3K inhibitor buparlisib in patients with BCBM (NCT02000882) and in melanoma brain metastases (NCT02452294). The mTOR inhibitor everolimus was recently assessed in combination with vinorelbine and trastuzumab in the treatment of HER2-positive, progressive breast cancer brain metastases (NCT01305941) and yielded low intracranial response rates (4%; ref. 38). Similarly, preliminary results of a recent phase Ib/II single-arm trial (NCT01783756) showed that the combination of everolimus,

lapatinib, and capecitabine for the treatment of HER2-positive breast cancer with brain metastases resulted in a 27% response rate in the brain after 12 weeks of treatment, highlighting the need for better therapies in this setting (39).

However, recent preclinical studies indicate that more favorable response rates can be achieved with dual inhibition of PI3K and mTOR (40), which further emphasizes the potential therapeutic advantages of GDC-0084. GDC-0084 has not been investigated in brain metastases patients to date.

We demonstrated *in vitro* that GDC-0084 induced apoptosis selectively in *PIK3CA*-MT BCBM cell lines at different magnitudes that corresponded to the extent of inhibition of molecular downstream targets of mTOR. These results were further validated with an isogenic epithelial breast cell line harboring a *PIK3CA* mutation. These findings are in line with a recent study in cSCC, which demonstrated that GDC-0084 dose dependently decreased cell viability, increased caspase-3 and caspase-9 activity and the proportion of cells in the G₀-1 phase, and decreased the proportion of cells in the S- and G₂M-phase (26).

In a patient-derived brain metastasis mouse model, we demonstrated that 15 mg/kg/day of GDC-0084 administered orally significantly inhibited tumor growth in a trastuzumab-resistant,

**Figure 4.**

GDC-0084 inhibits tumor growth in the brain *in vivo*. Tumor growth was analyzed via BLI and quantified as \log_{10} -transformed fold change of total flux (p/s). Imaging was performed 7 days after intracranial injection of tumor cells (pretreatment) and every 7 days thereafter until the 35th day postinjection. GDC-0084 significantly inhibited tumor growth compared with sham treatment in the mouse model using the *PIK3CA*-mutant cell line JIMT-1 BR-3 (A). No benefit was detected in the treatment cohort compared with sham controls in the *PIK3CA* wild-type MDA-MB-231 BrM2 model (B). Error bars represent SEM of \log_{10} -transformed total flux fold change values. Representative BLI images for treated and control mice of each model at the last day of imaging [JIMT-1 BR-3 (A) and MDA-MB-231 BrM2 (B)] are shown on right. See Supplementary Fig. S3 for changes in the flux for the individual animals over time.

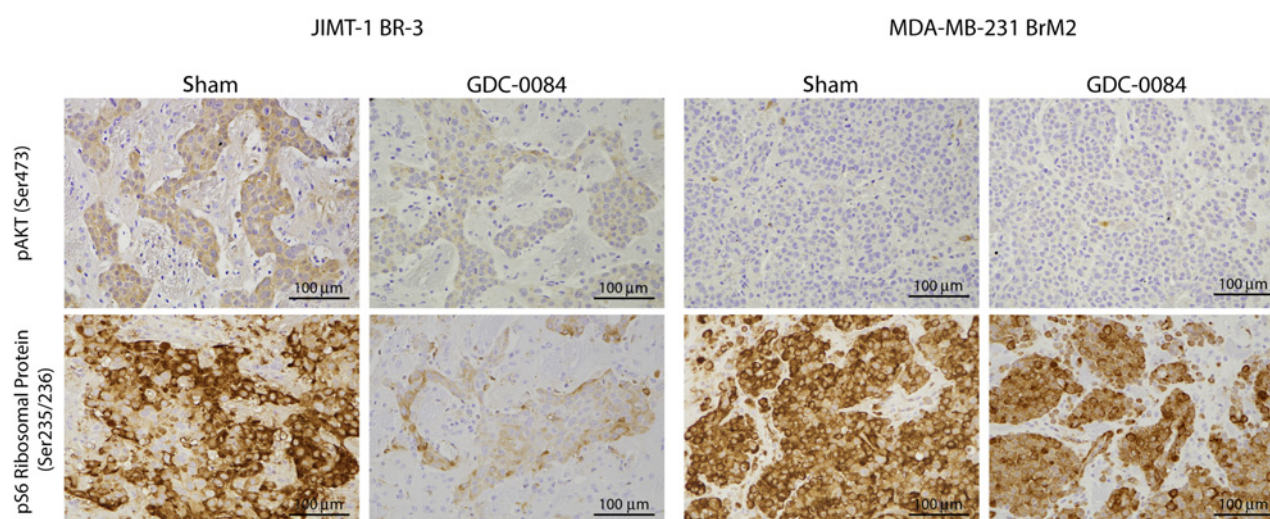
PIK3CA-MT cell line model and not a *PIK3CA*-WT cell line model. PI3K pathway inhibition within the brain was confirmed with IHC by reduction in signal intensity for pAkt and pS6 ribosomal protein in the *PIK3CA*-MT tumors treated with GDC-0084. These results are in accordance with previous *in vivo* results of GDC-0084 in a glioblastoma (27) and in a cSCC (26) model, which showed that GDC-0084 significantly reduced tumor volumes and resulted in reduced phosphorylation of downstream targets of the PI3K pathway (26, 27). Of note, mice in the cSCC study received a higher dose of either 25 or 50 mg/kg/day of GDC-0084 (26).

We investigated whether inhibition of the PI3K/Akt/mTOR pathway may cause a compensatory upregulation of the Ras/Raf/MAPK signaling cascade, as it has been previously shown (33, 34) and we did not observe GDC-0084-induced changes in the Ras/Raf/MAPK pathway signaling in both responsive and nonresponsive breast cancer models.

In summary, our findings highlight that the effect of GDC-0084 is genotype-selective, leading to a significant response in treated *PIK3CA*-MT breast cancer cell lines compared with WT. These results are of substantial translational relevance, particularly with regard to BCBM patients with resistance to HER2-directed treatment approaches (41). Recent preclinical data suggest that activation of the PI3K/Akt/mTOR pathway, including mechanisms like HER3 activation and PTEN loss, is a frequent mediator of drug-resistance toward HER2-targeted agents in the brain (41, 42). Combined PI3K and mTOR pathway blockade has been shown to overcome these resistance mechanisms (40) and may therefore present a promising treatment approach in affected patients in the future.

Our data therefore underscore the importance of brain-penetrant agents targeting the PI3K/Akt/mTOR pathway. The experimental results from this study provide valuable preclinical

Ippen et al.

**Figure 5.**

Photomicrographs illustrating pAkt (Ser473) and pS6 ribosomal protein (Ser235/236) expression in mouse brains harboring either JIMT-1 BR-3 or MDA-MB-231 BrM2 intracranial tumors, stratified by treatment with sham or GDC-0084. Staining for pAkt and pS6 ribosomal protein was considerably weaker in *PIK3CA*-mutant (JIMT-1 BR-3) tumors treated with GDC-0084 compared with sham. No clear differences in staining intensity were found in *PIK3CA* wild-type tumors (MDA-MB-231 BrM2) regardless of treatment.

support for the therapeutic efficacy of GDC-0084 in BCMB patients with dysregulated PI3K/mTOR signaling pathway. In future studies, *in vitro* and *in vivo* models in different genetic contexts will help identify additional biomarkers of response to PI3K inhibition. Although our preclinical results suggest a promising treatment option for affected patients with GDC-0084 as a single agent, there is an urgent need to explore combinatorial targeted treatment approaches to further improve intracranial tumor control and consequently, overall survival in breast BCMB patients. These findings warrant further validation in clinical trials to explore the therapeutic benefit of GDC-0084 in patients. A national multi-center trial is planned to evaluate the efficacy of GDC-0084 in brain metastases harboring *PIK3CA* mutations (Alliance study A071701).

Disclosure of Potential Conflicts of Interest

D.P. Cahill is a consultant/advisory board member for Merck and Lilly. P.K. Brastianos reports receiving speakers bureau honoraria from Merck, Genentech-Roche, and Tesaro, is a consultant/advisory board member for Lilly, Angiochem, and Roche, and reports receiving commercial research support from Merck. No potential conflicts of interest were disclosed by the other authors.

Authors' Contributions

Conception and design: F.M. Ippen, C.A. Alvarez-Breckenridge, G.R. Wojtkiewicz, S.L. Carter, D.P. Cahill, P.K. Brastianos
Development of methodology: F.M. Ippen, C.A. Alvarez-Breckenridge, B.M. Kuter, G.R. Wojtkiewicz, M. Martinez-Lage, S.L. Carter, P.K. Brastianos
Acquisition of data (provided animals, acquired and managed patients, provided facilities, etc.): F.M. Ippen, C.A. Alvarez-Breckenridge, B.M. Kuter,

A.L. Fink, I.V. Bihun, T. Penson, S.P. Schmidt, G.R. Wojtkiewicz, J. Ning, M. Martinez-Lage, P.K. Brastianos

Analysis and interpretation of data (e.g., statistical analysis, biostatistics, computational analysis): F.M. Ippen, C.A. Alvarez-Breckenridge, B.M. Kuter, M. Lastrapes, S.P. Schmidt, G.R. Wojtkiewicz, A. Giobbie-Hurder, M. Martinez-Lage, H. Wakimoto, P.K. Brastianos

Writing, review, and/or revision of the manuscript: F.M. Ippen, B.M. Kuter, G.R. Wojtkiewicz, M. Subramanian, A. Giobbie-Hurder, M. Martinez-Lage, D.P. Cahill, H. Wakimoto, P.K. Brastianos

Administrative, technical, or material support (i.e., reporting or organizing data, constructing databases): F.M. Ippen, B.M. Kuter, I.V. Bihun, M. Subramanian, P.K. Brastianos

Study supervision: F.M. Ippen, S.L. Carter, D.P. Cahill, H. Wakimoto, P.K. Brastianos

Other: P.K. Brastianos

Acknowledgments

F.M. Ippen is supported by the Deutsche Forschungsgemeinschaft (DFG, German Research Foundation- Projektnummer: 325246018). S. Carter is funded by NIH (R01 CA227156). P. Brastianos is funded by Breast Cancer Research Foundation, Susan G. Komen, American Brain Tumor Association, and NIH (R01 CA227156).

The costs of publication of this article were defrayed in part by the payment of page charges. This article must therefore be hereby marked *advertisement* in accordance with 18 U.S.C. Section 1734 solely to indicate this fact.

Received September 19, 2018; revised December 28, 2018; accepted February 18, 2019; published first February 22, 2019.

References

- Asher AL, Burri SH, Chahlavi A, Chang SM, Farace E, Fiveash JB, et al. The management of brain metastases. In: Schiff D, O'Neill BP, editors. Principles of neuro-oncology. 1st Edition. New York, NY: McGraw-Hill Medical Publishing Division; 2005. p.553–79.
- Eichler AF, Loeffler JS. Multidisciplinary management of brain metastases. *Oncologist* 2007;12:884–98.
- Soffietti R, Ducati A, Rudà R. Brain metastases. In: Aminoff MJ, Boller F, Swaab DF, editors. Handbook of clinical neurology. Elsevier; 2012. p. 747–55.
- Kocher M, Soffietti R, Abacioglu U, Villa S, Fauchon F, Baumert BG, et al. Adjuvant whole-brain radiotherapy versus observation after radiosurgery or surgical resection of one to three cerebral metastases: results of the EORTC 22952-26001 study. *J Clin Oncol* 2011;29:134–41.

5. Murray KJ, Scott C, Greenberg HM, Emami B, Seider M, Vora NL, et al. A randomized phase III study of accelerated hyperfractionation versus standard in patients with unresected brain metastases: a report of the Radiation Therapy Oncology Group (RTOG) 9104. *Int J Radiat Oncol Biol Phys* 1997; 39:571–4.
6. Shah R, Rosso K, Nathanson SD. Pathogenesis, prevention, diagnosis and treatment of breast cancer. *World J Clin Oncol* 2014;5:283–98.
7. Witzel I, Oliveira-Ferrer L, Pantel K, Müller V, Wikman H. Breast cancer brain metastases: biology and new clinical perspectives. *Breast Cancer Res* 2016;18:8.
8. Adamo B, Deal AM, Burrows E, Geradts J, Hamilton E, Blackwell KL, et al. Phosphatidylinositol 3-kinase pathway activation in breast cancer brain metastases. *Breast Cancer Res* 2011;13:R125.
9. Brastianos PK, Carter SL, Santagata S, Cahill DP, Taylor-Weiner A, Jones RT, et al. Genomic characterization of brain metastases reveals branched evolution and potential therapeutic targets. *Cancer Discov* 2015;5: 1164–77.
10. Saunus JM, Quinn MC, Patch AM, Pearson JV, Bailey PJ, Nones K, et al. Integrated genomic and transcriptomic analysis of human brain metastases identifies alterations of potential clinical significance. *J Pathol* 2015;237: 363–78.
11. Sadeghi N, Gerber DE. Targeting the PI3K pathway for cancer therapy. *Future Med Chem* 2012;4:1153–69.
12. de Gooijer MC, Zhang P, Buil LCM, Çitirikkaya CH, Thota N, Beijnen JH, et al. Buparlisib is a brain penetrable pan-PI3K inhibitor. *Sci Rep* 2018;8: 10784.
13. Lin NU. Breast cancer brain metastases: new directions in systemic therapy. *Ecancermedicallscience* 2013;7:307.
14. O'Reilly T, McSheehy PM, Kawai R, Kretz O, McMahon L, Brueggen J, et al. Comparative pharmacokinetics of RAD001 (everolimus) in normal and tumor-bearing rodents. *Cancer Chemother Pharmacol* 2010;65:625–39.
15. Brana I, LoRusso P, Baselga J, Heath EL, Patnaik A, Gendreau S, et al. A phase I dose-escalation study of the safety, pharmacokinetics (PK), and pharmacodynamics of XL765 (SAR245409), a PI3K/TORC1/TORC2 inhibitor administered orally to patients (pts) with advanced malignancies. *J Clin Oncol* 2010;28:15s (suppl; abstr 3030).
16. Cloughesy TF, Mischel PS, Omuro AMP, Prados M, Wen PY, Wu B, et al. Tumor pharmacokinetics (PK) and pharmacodynamics (PD) of SAR245409 (XL765) and SAR245408 (XL147) administered as single agents to patients with recurrent glioblastoma (GBM): an Ivy Foundation early-phase clinical trials consortium study. *J Clin Oncol* 2012;31:15s (suppl; abstr 2012).
17. Franz DN, Belousova E, Sparagana S, Bebin EM, Frost M, Kuperman R, et al. Efficacy and safety of everolimus for subependymal giant cell astrocytomas associated with tuberous sclerosis complex (EXIST-1): a multicentre, randomised, placebo-controlled phase 3 trial. *Lancet* 2013;381:125–32.
18. Koul D, Shen R, Kim YW, Kondo Y, Lu Y, Bankson J, et al. Cellular and in vivo activity of a novel PI3K inhibitor, PX-866, against human glioblastoma. *Neuro-oncol* 2010;12:559–69.
19. Liu TJ, Koul D, LaFortune T, Tiao N, Shen RJ, Maira SM, et al. NVP-BEZ235, a novel dual phosphatidylinositol 3-kinase/mammalian target of rapamycin inhibitor, elicits multifaceted antitumor activities in human gliomas. *Mol Cancer Ther* 2009;8:2204–10.
20. Paplomata E, O'Regan R. The PI3K/AKT/mTOR pathway in breast cancer: targets, trials and biomarkers. *Ther Adv Med Oncol* 2014;6:154–66.
21. Niessner H, Schmitz J, Tabatabai G, Schmid AM, Calaminus C, Sinnberg T, et al. PI3K pathway inhibition achieves potent antitumor activity in melanoma brain metastases in vitro and in vivo. *Clin Cancer Res* 2016; 22:5818–28.
22. Osswald M, Blaes J, Liao Y, Solecki G, Gommel M, Berghoff AS, et al. Impact of blood-brain barrier integrity on tumor growth and therapy response in brain metastases. *Clin Cancer Res* 2016;22:6078–87.
23. Chen G, Chakravarti N, Aardalen K, Lazar AJ, Tetzlaff MT, Wubbenhorst B, et al. Molecular profiling of patient-matched brain and extracranial melanoma metastases implicates the PI3K pathway as a therapeutic target. *Clin Cancer Res* 2014;20:5537–46.
24. Becker CM, Oberoi RK, McFarren SJ, Muldoon DM, Pafundi DH, Pokorny JL, et al. Decreased affinity for efflux transporters increases brain penetrance and molecular targeting of a PI3K/mTOR inhibitor in a mouse model of glioblastoma. *Neuro Oncol* 2015;17:1210–9.
25. Heffron TP, Ndubaku CO, Salphati L, Aliche B, Cheong J, Drobnick J, et al. Discovery of clinical development candidate GDC-0084, a brain penetrant inhibitor of PI3K and mTOR. *ACS Med Chem Lett* 2016;7:351–6.
26. Ding LT, Zhao P, Yang ML, Lv GZ, Zhao TL. GDC-0084 inhibits cutaneous squamous cell carcinoma cell growth. *Biochem Biophys Res Commun* 2018;503:1941–8.
27. Salphati L, Aliche B, Heffron TP, Shahidi-Latham S, Nishimura M, Cao T, et al. Brain distribution and efficacy of the brain penetrant PI3K inhibitor GDC-0084 in orthotopic mouse models of human glioblastoma. *Drug Metab Dispos* 2016;44:1881–9.
28. Jernström S, Hongisto V, Leivonen SK, Due EU, Tadele DS, Edgren H, et al. Drug-screening and genomic analyses of HER2-positive breast cancer cell lines reveal predictors for treatment response. *Breast Cancer (Dove Med Press)* 2017;9:185–98.
29. Kataoka Y, Mukohara T, Shimada H, Saijo N, Hirai M, Minami H. Association between gain-of-function mutations in PIK3CA and resistance to HER2-targeted agents in HER2-amplified breast cancer cell lines. *Ann Oncol* 2010;21:255–62.
30. Gustin JP, Karakas B, Weiss MB, Abukhdeir AM, Luring J, Garay JP, et al. Knockin of mutant PIK3CA activates multiple oncogenic pathways. *Proc Natl Acad Sci U S A* 2009;106:2835–40.
31. Iqbal A, Eckerd T, Bell J, Nakano I, Giles FJ, Cheng SY, et al. Targeting of glioblastoma cell lines and glioma stem cells by combined PIM kinase and PI3K-p110alpha inhibition. *Oncotarget* 2016;7:33192–201.
32. Khalil AA, Jameson MJ, Broaddus WC, Lin PS, Dever SM, Golding SE, et al. The influence of hypoxia and pH on bioluminescence imaging of luciferase-transfected tumor cells and xenografts. *Int J Mol Imaging* 2013;2013:287697.
33. Butler DE, Marlein C, Walker HF, Frame FM, Mann VM, Simms MS, et al. Inhibition of the PI3K/AKT/mTOR pathway activates autophagy and compensatory Ras/Raf/MEK/ERK signalling in prostate cancer. *Oncotarget* 2017;8:56698–713.
34. Yuen HF, Abramczyk O, Montgomery G, Chan KK, Huang YH, Sasazuki T, et al. Impact of oncogenic driver mutations on feedback between the PI3K and MEK pathways in cancer cells. *Biosci Rep* 2012;32:413–22.
35. O'Brien NA, Browne BC, Chow L, Wang Y, Ginther C, Arboleda J, et al. Activated phosphoinositide 3-kinase/AKT signaling confers resistance to trastuzumab but not lapatinib. *Mol Cancer Ther* 2010; 9:1489–502.
36. Leyland-Jones B. Human epidermal growth factor receptor 2-positive breast cancer and central nervous system metastases. *J Clin Oncol* 2009; 27:5278–86.
37. Wen PY, Cloughesy TF, Olivero A, Lu X, Mueller L, Coimbra AF, et al. A first-in-human phase 1 study to evaluate the brain-penetrant PI3K/mTOR inhibitor GDC-0084 in patients with progressive or recurrent high-grade glioma. *J Clin Oncol* 2016;34(15_suppl):2012.
38. Van Swearingen AED, Siegel MB, Deal AM, Sambade MJ, Hoyle A, Hayes DN, et al. LCCC 1025: a phase II study of everolimus, trastuzumab, and vinorelbine to treat progressive HER2-positive breast cancer brain metastases. *Breast Cancer Res Treat* 2018;171:637–48.
39. Hurvitz S, Singh R, Adams B, Taguchi JA, Chan D, Dichmann RA, et al. Phase Ib/II single-arm trial evaluating the combination of everolimus, lapatinib and capecitabine for the treatment of HER2-positive breast cancer with brain metastases (TRIO-US B-09). *Ther Adv Med Oncol* 2018;10: 1758835918807339.
40. Ni J, Ramkissoon SH, Xie S, Goel S, Stover DG, Guo H, et al. Combination inhibition of PI3K and mTORC1 yields durable remissions in mice bearing orthotopic patient-derived xenografts of HER2-positive breast cancer brain metastases. *Nat Med* 2016;22:723–6.
41. Kabraji S, Ni J, Lin NU, Xie S, Winer EP, Zhao JJ. Drug resistance in HER2-positive breast cancer brain metastases: blame the barrier or the brain? *Clin Cancer Res* 2018;24:1795–804.
42. Kodack DP, Askoxyllakis V, Ferraro GB, Sheng Q, Badeaux M, Goel S, et al. The brain microenvironment mediates resistance in luminal breast cancer to PI3K inhibition through HER3 activation. *Sci Transl Med* 2017;9:pii: eaal4682.

Clinical Cancer Research

The Dual PI3K/mTOR Pathway Inhibitor GDC-0084 Achieves Antitumor Activity in *PIK3CA*-Mutant Breast Cancer Brain Metastases

Franziska M. Ippen, Christopher A. Alvarez-Breckenridge, Benjamin M. Kuter, et al.

Clin Cancer Res 2019;25:3374-3383. Published OnlineFirst February 22, 2019.

Updated version	Access the most recent version of this article at: doi: 10.1158/1078-0432.CCR-18-3049
Supplementary Material	Access the most recent supplemental material at: http://clincancerres.aacrjournals.org/content/suppl/2019/02/22/1078-0432.CCR-18-3049.DC1

Cited articles	This article cites 40 articles, 14 of which you can access for free at: http://clincancerres.aacrjournals.org/content/25/11/3374.full#ref-list-1
-----------------------	--

E-mail alerts	Sign up to receive free email-alerts related to this article or journal.
Reprints and Subscriptions	To order reprints of this article or to subscribe to the journal, contact the AACR Publications Department at pubs@aacr.org .
Permissions	To request permission to re-use all or part of this article, use this link http://clincancerres.aacrjournals.org/content/25/11/3374 . Click on "Request Permissions" which will take you to the Copyright Clearance Center's (CCC) Rightslink site.